We are IntechOpen, the world's leading publisher of Open Access books Built by scientists, for scientists

4,800
Open access books available

122,000
International authors and editors

135M
Downloads

Our authors are among the

154
Countries delivered to

TOP 1%
most cited scientists

12.2%
Contributors from top 500 universities

CLARIVATE ANALYTICS BOOK CITATION INDEX INDEXED

WEB OF SCIENCE™

Selection of our books indexed in the Book Citation Index in Web of Science™ Core Collection (BKCI)

Interested in publishing with us?
Contact book.department@intechopen.com

Numbers displayed above are based on latest data collected.
For more information visit www.intechopen.com

Chapter 6

On Variable Structure Control Approaches to Semiactive Control of a Quarter Car System

Mauricio Zapateiro, Francesc Pozo and Ningsu Luo

Additional information is available at the end of the chapter

http://dx.doi.org/10.5772/50325

1. Introduction

Vehicle suspension systems are one of the most critical components of a vehicle and it have been a hot research topic due to their importance in vehicle performance. These systems are designed to provide comfort to the passengers to protect the chassis and the freigt [28]. However, ride comfort, road holding and suspension deflection are often conflicting and a compromise of the requirements must be considered. Among the proposed solutions, active suspension is an approach to improve ride comfort while keeping suspension stroke and tire deflection within an acceptable level [11, 21].

In semiactive suspension, the value of the damper coefficient can be controlled and can show reasonable performance as compared to that of an active suspension control. Besides, it does not require external energy. For instance, in the work by [18] a semiactive suspension control of a quarter-car model using a hybrid-fuzzy-logic-based controlled is developed and implemented. [23] formulated a force-tracking PI controller for an MR-damper controlled quarter-car system. The preliminary results showed that the proposed semiactive force tracking PI control scheme could provide effective control of the sprung mass resonance as well as the wheel-hop control. Furthermore, the proposed control yields lower magnitudes of mass acceleration in the ride zone. [25] designed a semi active suspension system using a magnetorhelogical damper. The control law was formulated following the sky-hook technique in which the direction of the relative velocity between the sprung and unsprung masses is compared to that of the velocity of the unsprung mass. Depending on this result, an on-off action is performed. [8] designed a semiactive static output H_∞ controller for a quarter car system equipped with a magnetorheological damper. In this case, the control law was formulated in order to regulate the vertical acceleration as a measure to keep passengers' comfort within acceptable limits. They also added a constraint in order to keep the transfer function form road disturbance to suspension deflection small enough to prevent excessive suspension bottoming.

Backstepping is a recursive design for systems with nonlinearities not constrained by linear bounds. The ease with which backstepping incorporated uncertainties and unknown parameters contributed to its instant popularity and rapid acceptance. Applications of this technique have been recently reported ranging from robotics to industry or aerospace [6, 7, 15, 22, 24]. Backstepping control has also been explored in some works about suspension systems. For example, [26] designed a semiactive backstepping control combined with neural network (NN) techniques for a system with MR damper. In that work, the controller was formulated for an experimental platform, whose MR damper was modeled by means of an artificial neural network. The control input was updated with a backstepping controller. On the other hand, [16] studied a hybrid control of active suspension systems for quarter-car models with two-degrees-of-freedom. This hybrid control was implemented by controlling the linear part with H_∞ techniques and the nonlinear part with an adaptive controller based on backstepping.

Some works on Quantitative Feedback Theory (QFT) applied to the control of suspension systems can be found in the literature. For instance, [1] analyzed H_∞ and QFT controllers designed for an active suspension system in order to account for the structured and unstructured uncertainties of the system. As a result, the vertical body acceleration in QFT-controlled is lower than that of the H_∞-controlled and its performance is superior. In the presence of a hydraulic actuator, the QFT-controlled system performance degrades but it is still comparable to that of the H_∞-control. [28] addressed a study leading to compare the performance of backstepping and QFT controllers in active and semiactive control of suspension systems. In this case, the nonlinearities were treated as uncertainties in the model so that the linear QFT could be applied to the control formulation. As a result, similar performances between both classes of controllers were achieved.

In this chapter, we will analyze three model-free variable structure controllers for a class of semiactive vehicle suspension systems equipped with MR dampers. The variable structure control (VSC) is a control scheme which is well suited for nonlinear dynamic systems [12]. VSC was firstly studied in the early 1950's for systems represented by single-input high-order differential equations. A rise of interest became in the 1970's because the robustness of VSC were step by step recognized. This control method can make the system completely insensitive to time-varying parameter uncertainties, multiple delayed state perturbations and external disturbances [17]. Nowadays, research and development continue to apply VSC control to a wide variety of engineering areas, such as aeronautics (guidance law of small bodies [29]), electric and electronic engineering (speed control of an induction motor drive [3]). By using this kind of controllers, it is possible to take the best out of several different systems by switching from one to the other. The first strategy that we propose in this work, σ_1, is based on the difference between the body angular velocity and the wheel angular velocity. The second strategy, σ_2, more complex, is based both on the difference between the body angular velocity and the wheel angular velocity, and on the difference between the body angular position and the wheel angular position. In this case, the resulting algorithm can be viewed as the clipped control in [9], but with some differences. Finally, the last strategy presented is based on a time variable depending on the absolute value of the difference between the body angular velocity and the wheel angular velocity, and on the difference between the body angular position and the wheel angular position. The study of the three

variable structure controllers will be complemented with the comparison of a model-based controller which has been successfully applied by the authors in other works: backstepping. As it was mentioned earlier, backstepping is well suited to this kind of problems because it can account for robustness and nonlinearities. It has been used by the authors to analyze this particular problem [28] with interesting results.

The chapter is organized as follows. Section 2 presents the mathematical details of the system to be controlled. In Section 3, the three variable structure controllers are developed. In Section 4, the backstepping control formulation details are outlined. Section 5 shows the numerical results, and in Section 6, the conclusions are drawn.

2. Suspension system model

The suspension system can be modeled as a quarter car model, as shown in Figure 1. The system can be viewed as a composition of two subsystems: the tyre subsystem and the suspension subsystem. The tyre subsystem is represented by the wheel mass m_u while the suspension subsystem consists of a sprung mass, m_s, that resembles the vehicle mass. This way of seeing the system will be useful later on when designing the model-based semi active controller. The compressibility of the wheel pneumatic is k_t, while c_s and k_s are the damping and stiffness of the uncontrolled suspension system. The quarter car model equations are given by:

$$m_s\dot{x}_4 + c_s(x_4 - x_2) + k_s x_3 - f_{\text{mr}} = 0 \tag{1}$$

$$m_u\dot{x}_2 - c_s(x_4 - x_2) - k_s x_3 + k_t x_1 + f_{\text{mr}} = 0 \tag{2}$$

where:

- x_1 is the tyre deflection
- x_2 is the unsprung mass velocity
- x_3 is the suspension deflection
- x_4 is the sprung mass velocity.

Taking x_1, x_2, x_3 and x_4 as state variables allows us to formulate the following state-space representation:

- Tyre subsystem:

$$\begin{aligned}\dot{x}_1 &= x_2 - d \\ \dot{x}_2 &= -\frac{k_t}{m_u}x_1 + \rho u\end{aligned} \tag{3}$$

- Suspension subsystem:

$$\begin{aligned}\dot{x}_3 &= -x_2 + x_4 \\ \dot{x}_4 &= -u\end{aligned} \tag{4}$$

where $\rho = m_s/m_u$, d is the velocity of the disturbance input and u is the acceleration input due to the damping subsystem. The input u is given by:

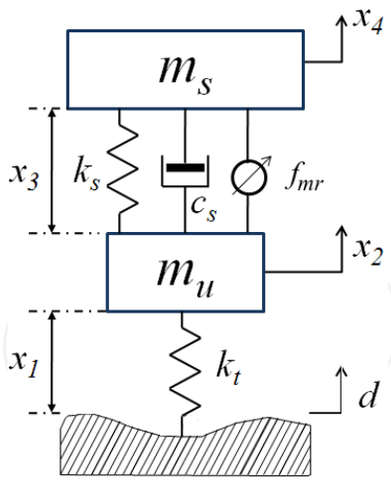

Figure 1. Quarter car suspension model

$$u = \frac{1}{m_s}(k_s x_3 + c_s(x_4 - x_2) - f_{\text{mr}}) \tag{5}$$

where f_{mr} is the damping force generated by the semiactive device. In this study, we assume that the semiactive device is magnetorheological (MR) damper. It is modeled according to the following Bouc-Wen model [19]:

$$f_{\text{mr}} = c_0(v)z_4 + k_0(v)z_3 + \alpha(v)\zeta \tag{6}$$

$$\dot{\zeta} = -\delta|z_4|\zeta|\zeta|^{n-1} - \beta z_4|\zeta|^n + \kappa z_4 \tag{7}$$

where ζ is an evolutionary variable that describes the hysteretic behavior of the damper, z_4 is the piston velocity, z_3 is the piston deflection and v is a voltage input that controls the current that generates the magnetic field; δ, β, κ and n are parameters that are chosen so to adjust the hysteretic dynamics of the damper; $c_0(v) = c_{0a} + c_{0b}v$ represents the voltage-dependent damping, $k_0(v) = k_{0a} + k_{0b}v$ represents the voltage-dependent stiffness and $\alpha(v) = \alpha_a + \alpha_b v$ is a voltage-dependent scaling factor.

3. Variable structure controller formulation

Feedback control radically alters the dynamics of a system: it affects its natural frequencies, its transient response as well as its stability. The MR damper of the quarter-car model considered in this study is voltage-controlled, so the voltage (v) is updated by a feedback control loop.

It is well known that the force generated by the MR damper cannot be commanded; only the voltage v applied to the current driver for the MR damper can be directly changed. One of the first control approaches involving an MR damper was proposed by [9] and called it clipped optimal control. In this approach, the command voltage takes one of two possible values: zero or the maximum. This is chosen according to the following algorithm:

$$v = V_{\max} H\{(f_{\text{d}} - f_{\text{mr}})f_{\text{mr}}\} \tag{8}$$

$$= \frac{V_{\max}}{2}\left[\text{sgn}\left[(f_{\text{d}} - f_{\text{mr}})f_{\text{mr}}\right] + 1\right], \tag{9}$$

where $V_{\max}$ is the maximum voltage to the current driver associated with saturation of the magnetic field in the MR damper, $H(\cdot)$ is the Heaviside step function, f_{d} is the desired control force and f_{mr} is the measured force of the MR damper.

The sign part of equation (9) can be transformed in the following way:

$$\begin{aligned}
\operatorname{sgn}\left[\left(f_{\mathrm{d}}-f_{\mathrm{mr}}\right)f_{\mathrm{mr}}\right] &= \begin{cases} 1, & \left(f_{\mathrm{d}}-f_{\mathrm{mr}}\right)f_{\mathrm{mr}}>0 \\ -1, & \left(f_{\mathrm{d}}-f_{\mathrm{mr}}\right)f_{\mathrm{mr}}<0 \end{cases} \\
&= \begin{cases} 1, & \left[\left(f_{\mathrm{d}}-f_{\mathrm{mr}}\right)>0 \text{ and } f_{\mathrm{mr}}>0\right] \text{ or } \left[\left(f_{\mathrm{d}}-f_{\mathrm{mr}}\right)<0 \text{ and } f_{\mathrm{mr}}<0\right] \\ -1, & \left[\left(f_{\mathrm{d}}-f_{\mathrm{mr}}\right)>0 \text{ and } f_{\mathrm{mr}}<0\right] \text{ or } \left[\left(f_{\mathrm{d}}-f_{\mathrm{mr}}\right)<0 \text{ and } f_{\mathrm{mr}}>0\right] \end{cases} \\
&= \begin{cases} 1, & \left[f_{\mathrm{d}}>f_{\mathrm{mr}} \text{ and } f_{\mathrm{mr}}>0\right] \text{ or } \left[f_{\mathrm{d}}<f_{\mathrm{mr}} \text{ and } f_{\mathrm{mr}}<0\right] \\ -1, & \left[f_{\mathrm{d}}>f_{\mathrm{mr}} \text{ and } f_{\mathrm{mr}}<0\right] \text{ or } \left[f_{\mathrm{d}}<f_{\mathrm{mr}} \text{ and } f_{\mathrm{mr}}>0\right] \end{cases} \\
&= \begin{cases} 1, & f_{\mathrm{d}}>f_{\mathrm{mr}} \text{ and } f_{\mathrm{mr}}>0 \\ 1, & f_{\mathrm{d}}<f_{\mathrm{mr}} \text{ and } f_{\mathrm{mr}}<0 \\ -1, & f_{\mathrm{d}}>f_{\mathrm{mr}} \text{ and } f_{\mathrm{mr}}<0 \\ -1, & f_{\mathrm{d}}<f_{\mathrm{mr}} \text{ and } f_{\mathrm{mr}}>0 \end{cases}
\end{aligned}$$

Finally, the full expression in equation (9) can be rewritten as a piecewise function in the following way:

$$\frac{V_{\max}}{2}\left[\operatorname{sgn}\left[\left(f_{\mathrm{d}}-f_{\mathrm{mr}}\right)f_{\mathrm{mr}}\right]+1\right] = \begin{cases} V_{\max}, & f_{\mathrm{d}}>f_{\mathrm{mr}} \text{ and } f_{\mathrm{mr}}>0 \\ V_{\max}, & f_{\mathrm{d}}<f_{\mathrm{mr}} \text{ and } f_{\mathrm{mr}}<0 \\ 0, & f_{\mathrm{d}}>f_{\mathrm{mr}} \text{ and } f_{\mathrm{mr}}<0 \\ 0, & f_{\mathrm{d}}<f_{\mathrm{mr}} \text{ and } f_{\mathrm{mr}}>0 \end{cases}$$

This algorithm for selecting the command signal is graphically represented in Figure 2. More precisely, the shadowed area in Figure 2 is the area where $f_{\mathrm{d}}>f_{\mathrm{mr}}$ and $f_{\mathrm{mr}}>0$, or $f_{\mathrm{d}}<f_{\mathrm{mr}}$ and $f_{\mathrm{mr}}<0$. Note that in that particular work, they used the voltage as the control signal because that is the way that current driver can be controlled.

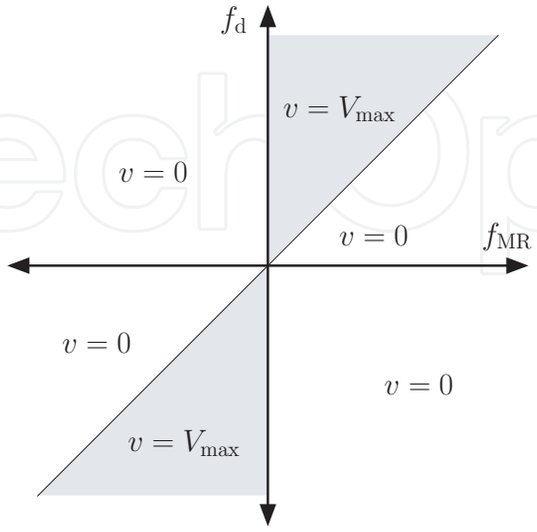

Figure 2. Graphical representation of the algorithm in equation (8) for selecting the command signal.

In this paper we consider the same idea of changing the voltage. This control signal is computed according to the following control strategies, computed as a function of the sprung mass velocity (x_4), the unsprung mass velocity (x_2), and the suspension deflection (x_3):

$$\sigma_1: \quad v(x_2, x_4) = \frac{V_{\max}}{2}\left[\text{sgn}(x_4 - x_2) + 1\right] \tag{10}$$

$$\sigma_2: \quad v(x_2, x_3, x_4) = \frac{V_{\max}}{2}\left[\text{sgn}\left(\text{sgn}(x_4 - x_2) + x_3\right) + 1\right] \tag{11}$$

$$\sigma_3: \quad v(x_2, x_4) = \frac{V_{\max}}{2}[\text{sgn}(r) + 1],\ \frac{dr}{dt} = -100r|x_4 - x_2| - 10(x_4 - x_2) \tag{12}$$

Variable structure controllers (VSC) are a very large class of robust controllers [10]. The distinctive feature of VSC is that the structure of the system is intentionally changed according to an assigned law. This can be obtained by switching on or cutting off feedback loops, scheduling gains and so forth. By using VSC, it is possible to take the best out of several different systems (more precisely structures), by switching from one to the other. The control law defines various regions in the phase space and the controller switches between a structure and another at the boundary between two different regions according to the control law.

The three strategies presented in this section can be viewed as variable structure controllers, since the value of the control signal is set to be zero or one, as can be seen in the following transformations:

$$\sigma_1: \quad v(x_2, x_4) = \frac{V_{\max}}{2}\left[\text{sgn}(x_4 - x_2) + 1\right] \tag{13}$$

$$= \begin{cases} 0, & \text{if } \Delta\omega < 0, \\ V_{\max}, & \text{if } \Delta\omega \geq 0 \end{cases} \tag{14}$$

$$\sigma_2: \quad v(x_2, x_3, x_4) = \frac{V_{\max}}{2}\left[\text{sgn}\left(\text{sgn}(x_4 - x_2) + x_3\right) + 1\right] \tag{15}$$

$$= \begin{cases} 0, & \text{if } \Delta\omega < 0,\ x_3 < 1\ (\text{region IV}), \\ 0, & \text{if } \Delta\omega > 0,\ x_3 < -1\ (\text{region I}), \\ V_{\max}, & \text{if } \Delta\omega < 0,\ x_3 \geq 1\ (\text{region II}), \\ V_{\max}, & \text{if } \Delta\omega \geq 0,\ x_3 \geq -1\ (\text{region III}) \end{cases} \tag{16}$$

$$\sigma_3: \quad v(x_2, x_4) = \frac{V_{\max}}{2}[\text{sgn}(r) + 1] \tag{17}$$

$$= \begin{cases} 0, & \text{if } r < 0, \\ V_{\max}, & \text{if } r \geq 0 \end{cases},\ \frac{dr}{dt} = -100r|x_4 - x_2| - 10(x_4 - x_2) \tag{18}$$

where $\Delta\omega = x_4 - x_2$. In Figure 3 we hace depicted the graphical representation of the strategy σ_2 for selecting the command signal.

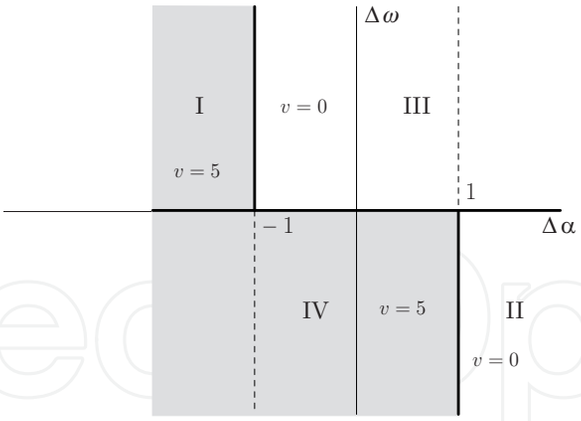

Figure 3. Graphical representation of the strategy σ_2 for selecting the command signal.

Semi-active control have two essential characteristics. The first is that the these devices offer the adaptability of active control devices without requiring the associated large power sources. The second is that the device cannot inject energy into the system; hence semi-active control devices do not have the potential to destabilize (in the bounded input–bounded output sense) the system [20]. As a consequence, the stability of the closed-loop system is guaranteed.

4. Backstepping controller formulation

In this section we present the formulation of a model-based controller. The objective, as explained in the Introduction, is to make a comparison between this model-based controller and the VSC controllers. We will appeal to the backstepping technique that has been developed in previous works for this kind of systems.The objective is to design an adaptive backstepping controller to regulate the suspension deflection with the aid of an MR damper thus providing safety and comfort while on the road. The adaptive backstepping controller will be designed in such a way that, for a given $\gamma > 0$, the state-dependent error variables e_1 and e_2 (to be defined later) accomplish the following H_∞ performance $J_\infty < 0$:

$$J_\infty = \int_0^\infty (\mathbf{e}^T \mathbf{R} \mathbf{e} - \gamma^2 \mathbf{w}^T \mathbf{w}) dt \tag{19}$$

where $\mathbf{e} = (e_1, e_2)^{\mathrm{T}}$ is a vector of controlled signals, $\mathbf{R} = \mathrm{diag}\{r_1, r_2\}$ is a positive definite matrix and $\mathbf{w}$ is an energy-bounded disturbance.

In order to formulate the backstepping controller, the state space model (3) - (4) must be first written in strict feedback form [14]. Therefore, the following coordinate transformation is performed [13]:

$$\begin{aligned} z_1 &= x_1 + \frac{\rho}{\rho+1} x_3 \\ z_2 &= \frac{1}{\rho+1} x_2 + \frac{\rho}{\rho+1} x_4 \\ z_3 &= x_3 \\ z_4 &= -x_2 + x_4 \end{aligned} \tag{20}$$

The system, represented in the new coordinates, is given by:

- Tyre subsystem:

$$\begin{aligned}\dot{z}_1 &= z_2 - d \\ \dot{z}_2 &= -k_t[m_u(\rho+1)]^{-1}z_1 + \rho k_t[m_u(\rho+1)^2]^{-1}z_3\end{aligned} \tag{21}$$

- Suspension subsystem:

$$\begin{aligned}\dot{z}_3 &= z_4 \\ \dot{z}_4 &= k_t m_u^{-1} z_1 - k_t\rho[m_u(\rho+1)]^{-1}z_3 - (\rho+1)u\end{aligned} \tag{22}$$

Substitution of the expression for u (5) into (22) yields:

$$\begin{aligned}\dot{z}_3 =& z_4 \\ \dot{z}_4 =& k_t m_u^{-1} z_1 - k_t\rho[m_u(\rho+1)]^{-1}z_3 - \\ & (\rho+1)m_s^{-1}[k_s x_3 + c_s(x_4 - x_2) - f_{\mathrm{mr}}] \\ =& -[k_t m_s\rho(\rho+1)^{-1} + (\rho+1)k_s m_u](m_u m_s)^{-1}z_3 + \\ & k_t m_u^{-1} z_1 - (\rho+1)m_s^{-1}c_s z_4 + (\rho+1)m_s^{-1}f_{\mathrm{mr}} \\ =& d_i - a_k z_3 - a_c z_4 + a_f f_{\mathrm{mr}}\end{aligned} \tag{23}$$

where $a_k = [k_t m_s\rho(\rho+1)^{-1} + (\rho+1)k_s m_u](m_u m_s)^{-1}$, $a_c = (\rho+1)m_s^{-1}c_s$ and $a_f = (\rho+1)m_s^{-1}$; $d_i = k_t m_s^{-1} z_1$ reflects the fact that the disturbance enters to the suspension subsystem through the tyre subsystem.

Assume that a_k and a_c in (23) are uncertain constant parameters whose estimated values are $\hat{a}_k$ and $\hat{a}_c$, respectively. Thus, the errors between the estimates and the actual values are given by:

$$\tilde{a}_k = a_k - \hat{a}_k \tag{24}$$

$$\tilde{a}_c = a_c - \hat{a}_c \tag{25}$$

Let $a_d = k_t[m_u(\rho+1)]^{-1}$, $a_n = \rho k_t[m_u(\rho+1)^2]^{-1}$ and $a_m = k_t m_u^{-1}$. From (21) - (22), it can be shown that the transfer functions from $d(t)$ and $f_{\mathrm{mr}}(t)$ to $z_1(t)$ are:

$$\frac{Z_1(s)}{D(s)} = \frac{-s(s^2 + a_c s + a_k)}{s^4 + a_c s^3 + (a_d + a_k)s^2 + a_d a_c s + a_d a_k - a_m a_n} \tag{26}$$

$$\frac{Z_1(s)}{F_{\mathrm{mr}}(s)} = \frac{a_n a_f}{s^4 + a_c s^3 + (a_d + a_k)s^2 + a_d a_c s + a_d a_k - a_m a_n} \tag{27}$$

If the poles of the transfer functions (26) and (27) are in the left side of the s plane, then we can guarantee the bounded input - bounded output (BIBO) stability of $Z_1(s)$ for any bounded input $D(s)$ and $F_{\mathrm{mr}}(s)$. Thus, the disturbance input $d_i(t)$ in (23) is also bounded. This boundedness condition will be necessary later in the controller stability condition.

Finally, since $d_i(t)$ is the only disturbance input to the suspension subsystem, the vector $\mathbf{w}$ of the H_∞ performance objective as given in (19) becomes:

$$J_\infty = \int_0^\infty (\mathbf{e}^T\mathbf{R}\mathbf{e} - \gamma^2 d_i^2)dt \tag{28}$$

In order to begin with the adaptive backstepping design, we firstly define the following error variable and its derivative:

$$e_1 = z_3 \tag{29}$$

$$\dot{e}_1 = \dot{z}_3 = z_4 \tag{30}$$

Now, the following Lyapunov function candidate is chosen:

$$V_1 = \frac{1}{2}e_1^2 \tag{31}$$

whose first-order derivative is:

$$\dot{V}_1 = e_1\dot{e}_1 = e_1 z_4 \tag{32}$$

Equation (30) can be stabilized with the following virtual control input:

$$z_{4d} = -r_1 e_1 \tag{33}$$

$$\dot{z}_{4d} = -r_1\dot{e}_1 = -r_1 z_4 \tag{34}$$

where $r_1 > 0$. Now define a second error variable and its derivative:

$$e_2 = z_4 - z_{4d} \tag{35}$$

$$\dot{e}_2 = \dot{z}_4 - \dot{z}_{4d} \tag{36}$$

Therefore,

$$\dot{V}_1 = e_2 z_4 = e_1(e_2 - r_1 e_1) = e_1 e_2 - r_1 e_1^2 \tag{37}$$

On the other hand, the derivatives of the errors of the uncertain parameter estimations are given by:

$$\dot{\tilde{a}}_k = -\dot{\hat{a}}_k \tag{38}$$

$$\dot{\tilde{a}}_c = -\dot{\hat{a}}_c \tag{39}$$

Now, an augmented Lyapunov function candidate is chosen:

$$V = V_1 + \frac{1}{2}e_2^2 + \frac{1}{2r_k}\tilde{a}_k^2 + \frac{1}{2r_c}\tilde{a}_c^2 \tag{40}$$

Thus, by using (35) - (39) and the fact that $a_k = \tilde{a}_k + \hat{a}_k$ and $a_c = \tilde{a}_c + \hat{a}_c$, the derivative of V yields:

$$\begin{aligned}
\dot{V} =& e_1\dot{e}_1 + e_2\dot{e}_2 + r_k^{-1}\tilde{a}_k\dot{\tilde{a}}_k + r_c^{-1}\tilde{a}_c\dot{\tilde{a}}_c \\
=& e_1 e_2 - r_1 e_1^2 + e_2 d_i - a_k z_3 e_2 - a_c z_4 e_2 + a_f f_{\mathrm{mr}} e_2 - r_1 z_4 e_2 - r_k^{-1}\tilde{a}_k\dot{\hat{a}}_k - r_c^{-1}\tilde{a}_c\dot{a}_c \\
=& e_1 e_2 - r_1 e_1^2 + e_2 d_i + a_f f_{\mathrm{mr}} e_2 - r_1 z_4 e_2 - r_k^{-1}\tilde{a}_k\dot{\hat{a}}_k - (\tilde{a}_k + \hat{a}_k) z_3 e_2 - (\tilde{a}_c + \hat{a}_c) z_4 e_2 - r_c^{-1}\tilde{a}_c\dot{\hat{a}}_c \\
=& e_1 e_2 - r_1 e_1^2 + e_2 d_i - \tilde{a}_k(z_3 e_3 + r_k^{-1}\dot{\hat{a}}_k) - \hat{a}_k z_3 e_2 - \tilde{a}_c(z_4 e_2 + r_c^{-1}\dot{\hat{a}}_c) - \hat{a}_c z_4 e_2 + a_f + \\
& f_{\mathrm{mr}} e_2 - r_1 z_4 e_2
\end{aligned} \tag{41}$$

Now consider the following adaptation laws:

$$z_3 e_1 + r_k^{-1}\dot{\hat{a}}_k = 0 \tag{42}$$

$$z_4 e_2 + r_c^{-1}\dot{\hat{a}}_c = 0 \tag{43}$$

Substitution of (42) and (43) into (41) yields:

$$\dot{V} = -r_1 e_1^2 + e_2 d_i + e_2(e_1 - \hat{a}_k z_3 - \hat{a}_c z_4 + a_f f_{\text{mr}} - r_1 z_4) \tag{44}$$

By choosing the following control law:

$$f_{\text{mr}} = -\frac{e_1 - \hat{a}_k z_3 - \hat{a}_c z_4 - r_1 z_4 + r_2 e_2 + e_2(2\gamma)^{-2}}{a_f} \tag{45}$$

with $\gamma > 0$ and $r_2 > 0$, we get:

$$\begin{aligned}
\dot{V} &= -r_1 e_1^2 + e_2 d_i - r_2 e_2^2 - e_2^2(2\gamma)^{-2} \\
&= -r_1 e_1^2 + e_2 d_i - r_2 e_2^2 - e_2^2(2\gamma)^{-2} + \gamma^2 d_i^2 - \gamma^2 d_i^2 \\
&= -r_1 e_1^2 - r_2 e_2^2 + \gamma^2 d_i^2 - (\gamma d_i - e_2(2\gamma)^{-2})^2 \\
\dot{V} &\leq -r_1 e_1^2 - r_2 e_2^2 + \gamma^2 d_i^2
\end{aligned} \tag{46}$$

The objective of guaranteeing global boundedness of trajectories is equivalently expressed as rendering $\dot{V}$ negative outside a compact region. As stated earlier, the disturbance input d_i is bounded as long as the poles of the transfer functions (26) and (27) are in the left side of the s plane. When this is the case, the boundedness of the input disturbance d_i guarantees the existence of a small compact region $D \subset \mathbb{R}^2$ (depending on γ and d_i itself) such that $\dot{V}$ is negative outside this set. More precisely, when $r_1 e_1^2 + r_2 e_2^2 < \gamma^2 d_i^2$, $\dot{V}$ is positive and then the error variables are increasing values. Finally, when the expression $r_1 e_1^2 + r_2 e_2^2$ is greater than $\gamma^2 d_i^2$, $\dot{V}$ is then negative. This implies that all the closed-loop trajectories have to remain bounded, as we wanted to show. Now, under zero initial conditions, from 46 we can write:

$$\int_0^\infty \dot{V}\, dt \leq -\int_0^\infty r_1 e_1^2\, dt - \int_0^\infty r_2 e_2^2\, dt + \int_0^\infty \gamma^2 d_i^2\, dt \tag{47}$$

or, equivanlently,

$$V|_{t=\infty} - V|_{t=0} \leq -\int_0^\infty \mathbf{e}^T \mathbf{R}\mathbf{e}\, dt + \gamma^2 \int_0^\infty d_i^2\, dt \tag{48}$$

Then, it can be shown that

$$J_\infty = \int_0^\infty (\mathbf{e}^T \mathbf{R}\mathbf{e} - \gamma^2 d_i^2)\, dt \leq -V|_{t=\infty} \leq 0 \tag{49}$$

Thus, the adaptive backstepping controller satisfies both the H_∞ performance and the asymptotic stability of the system.

The control force given by (45) can be used to drive an actively controlled damper. However, the fact that semiactive devices cannot inject energy into a system, makes necessary the modification of this control law in order to implement it with a semiactive damper; that is, semiactive dampers cannot apply force to the system, only absorb it. There are different ways to perform this [2, 27]. In this work, we will calculate the MR damper voltage making use of its mathematical model. Thus, the following control law is proposed:

$$v = \frac{-e_1 - \hat{a}_z z_3 + \hat{a}_c z_4 + r_1 z_4 - r_2 e_2 - e_2 (2\gamma)^{-2} + a_f (c_{0a} z_4 + k_{0a} z_3 + \alpha_a \zeta)}{a_f (c_{0b} z_4 + k_{0b} z_3 + \alpha_b \zeta)} \tag{50}$$

provided that $a_f(c_{0b}z_4 + k_{0b}z_3 + \alpha_b\zeta) \neq 0$; otherwise, $v = 0$.

The same process followed to obtain the control law (45) can be used to demonstrate that the control law (4) does stabilize the system. Begin by replacing (6) into (44) in order to obtain:

$$\begin{aligned} \dot{V} = & -r_1 e_1^2 + e_2 d_i + e_2 [e_1 - \hat{a}_k z_3 - \hat{a}_c z_4 + a_f (c_{0a} z_4 + k_{0a} z_3 + \alpha_a \zeta) + \\ & a_f (c_{0b} z_4 + k_{0b} z_3 + \alpha_b \zeta) v - r_1 z_4] \end{aligned} \tag{51}$$

Thus, by replacing the control law of (4) into (51) we also get $\dot{V} \leq -r_1 e_1^2 - r_2 e_2^2 + \gamma^2 d_i^2$ and, as previously stated, the stability of the system is guaranteed.

Finally, we can write the control law in terms of the state variables as follows:

$$\begin{aligned} v = & \frac{\left(-\hat{a}_c - r_1 + r_2 + (2\gamma)^{-2} + a_f c_{0a}\right) x_2 + \left(-1 - \hat{a}_z - r_1 r_2 + r_1 (2\gamma)^{-2} + a_f k_{0a}\right) x_3}{-a_f c_{0b} x_2 + a_f k_{0b} x_3 + a_f c_{0b} x_4 + a_f \alpha_b \zeta} + \\ & \frac{\left(\hat{z}_c + r_1 - r_2 - (2\gamma)^{-2} + a_f c_{0a}\right) x_4 + a_f \alpha_a \zeta}{-a_f c_{0b} x_2 + a_f k_{0b} x_3 + a_f c_{0b} x4 + a_f \alpha_b \zeta} \end{aligned} \tag{52}$$

5. Numerical simulations

In this section we will analyze the performance results obtained form simulations performed in Matlab/SImulink. The numerical values of the model that we used in this study. Thus: α_a = 332.7 N/m, α_b = 1862.5 N·V/m, c_{0a} = 7544.1 N·s/m, c_{0b} = 7127.3 N·s·V/m, k_0a = 11375.7 N/m, k_{0b} = 14435.0 N·V/m, δ = 4209.8 m^{-2}, κ = 10246 and n = 2. This is a scaled version of the MR damper found in [5]. The parameter values of the suspension system are [13]: m_s=11739 kg, m_u=300 kg, k_s=252000 N/m, c_s=10000 N·s/m and k_t=300000 N/m. In order to facilitate the analysis, we will quantify the performance results by means of the indices shown in Table 1. Indices J_1 - J_3 show the ratio between the peak response of the controlled suspension system (displacement, velocity and acceleration) and that of the uncontrolled system. Indices J_4 - J_6 are the normalized ITSE (integral of the time squared error) signals that indicate how much the displacement, velocity and acceleration are attenuated compared to the uncontrolled case. Index J_7 is the relative maximum control effort with respect to the weight of the suspension system. Small indices indicate good control performance. Two scenarios are considered: an uneven road, simulated by random vibrations and the presence of a bump on the road.

We assume that the car has laser sensors that allow us to read the position of the sprung and unsprung masses. Since the velocities are needed for control implementation, these are obtained by first low-pass filtering the displacement readings and then applying a filter of the form $\frac{s}{(\lambda s+1)^q}$ that approximates the derivative of the signal. In this filter, λ is a sufficiently small constant that can be obtained from the ratio between the two-norm of the second derivative of the signal and the noise amplitude; q is the order of the filter which should be at lest equal to 2. Choosing parameters this way, allows for minimizing the error between the real and the estimated signal derivatives [4].

Index	Definition
$J_1 = \frac{max\|x_3(t)\|_{cont}}{max\|x_3(t)\|_{unc}}$	Norm. peak suspension deflection.
$J_2 = \frac{max\|x_4(t)\|_{cont}}{max\|x_4(t)\|_{unc}}$	Norm. peak sprung mass velocity.
$J_3 = \frac{max\|\dot{x}_4(t)\|_{cont}}{max\|\dot{x}_4(t)\|_{unc}}$	Norm. peak sprung mass acceleration.
$J_4 = \frac{\int_0^T t x_{3cont}^2(t)\,dt}{\int_0^T t x_{3unc}^2(t)\,dt}$	Norm. suspension deflection ITSE.
$J_5 = \frac{\int_0^T t x_{4cont}^2(t)\,dt}{\int_0^T t x_{4unc}^2(t)\,dt}$	Norm. sprung mass velocity ITSE.
$J_6 = \frac{\int_0^T t \dot{x}_{4cont}^2(t)\,dt}{\int_0^T t \dot{x}_{4unc}^2(t)\,dt}$	Norm. sprung mass acceleration ITSE.
$J_7 = \frac{max\|f_{mr}(t)\|}{w_s}$	Maximum control effort.

Table 1. Performance indices.

In the first scenario, the unevenness of the road was simulated by random vibration, as shown in Figure 4. This figure also compares the performance of the three σ controllers. What we can see for this figure, is that the three VSC controllers perform in a similar way and satisfactorily control the deflection of the tyre subsystem. In Figure 5, we see the performance of the same controllers at regulating the suspension deflection. Once again, the three controllers accomplish the objective in a similar way. This visual observations can be confirmed by analyzing the performance indices of Table 2. In Figures 6 and 7, we can see a comparison of the σ_3 controller and the backstepping controller. A notable superiority of the VSC controller is observed over the backstepping controller. It can be due to the fact that this kind of controllers are more sensitive to the fast-changing dynamics of a signal, in this case, the velocity, which can make it react faster. The performance indices of Table 2 also show that it is harder for the backstepping controller to keep the peak acceleration, velocity and displacement under acceptable limits, despite its control effort is much higher than that of the VSC controllers.

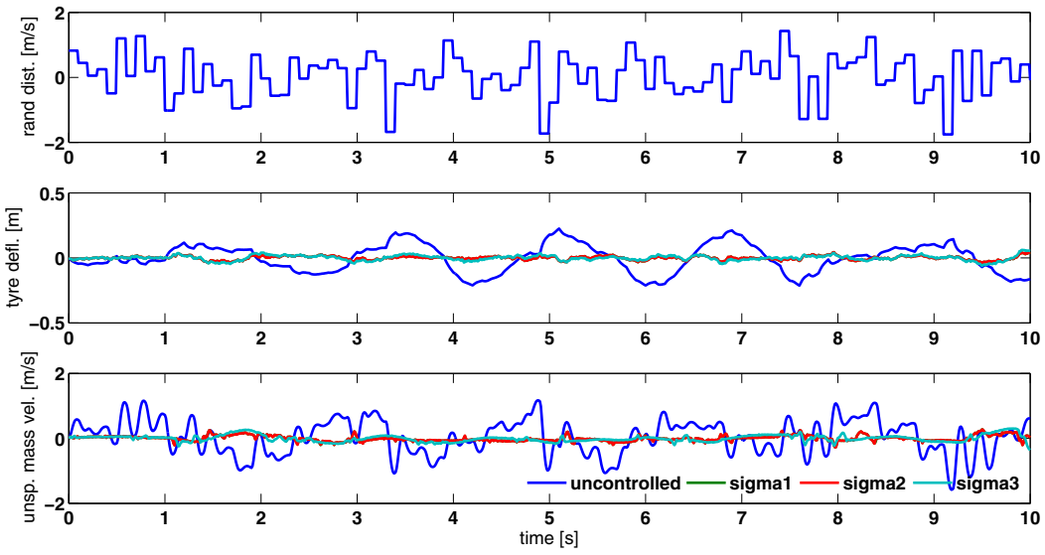

Figure 4. Uneven road disturbance and tyre subsystem response.

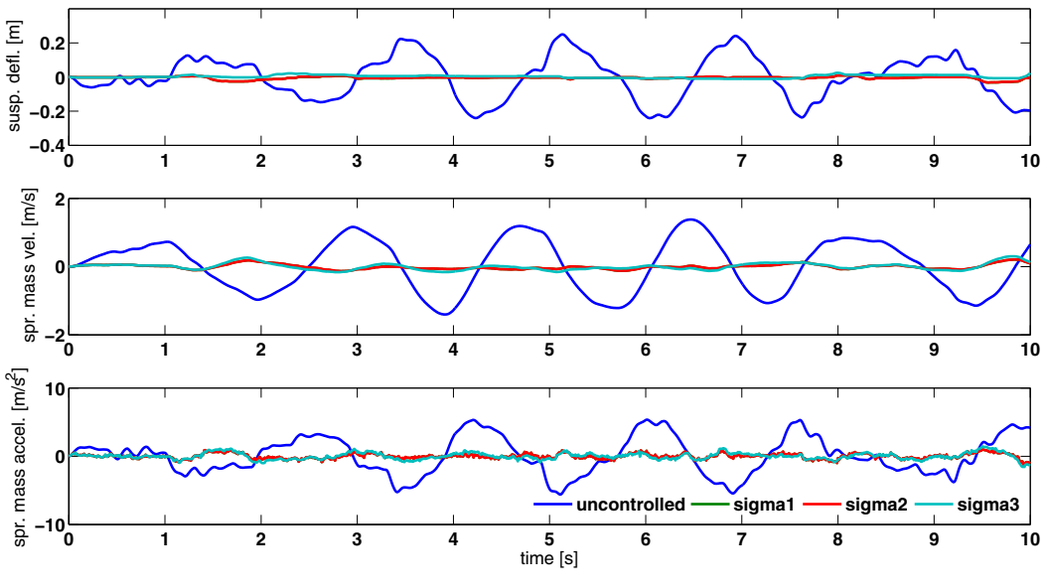

Figure 5. Uneven road disturbance and tyre subsystem response.

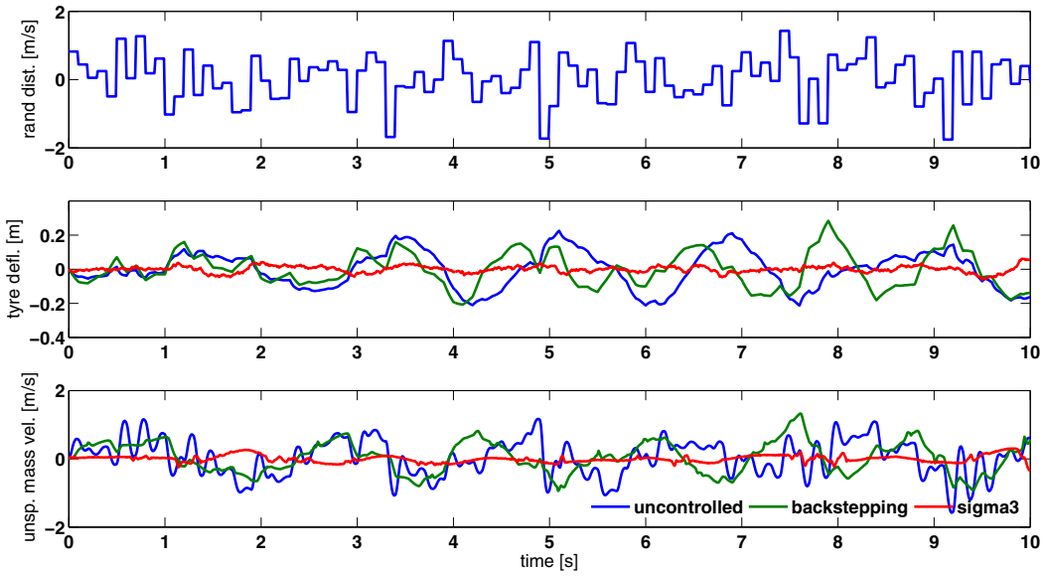

Figure 6. Uneven road disturbance and tyre subsystem response.

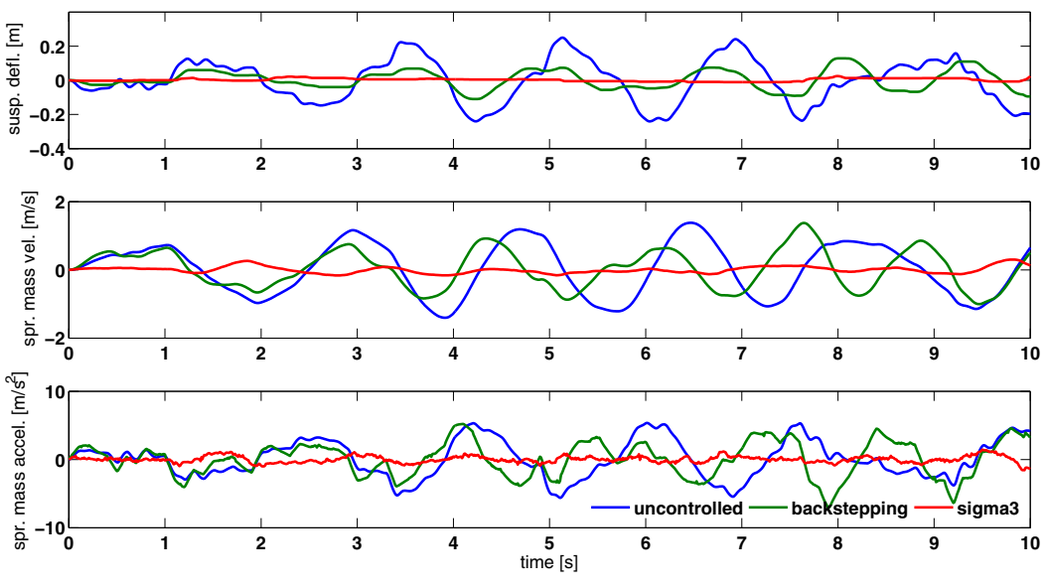

Figure 7. Uneven road disturbance and car subsystem response.

Index	σ_1	σ_2	σ_3	Backstepping
J_1	0.1288	0.1280	0.0993	0.5144
J_2	0.1485	0.1488	0.2157	0.9800
J_3	0.2205	0.2803	0.2803	1.2586
J_4	0.0059	0.0058	0.0053	0.2317
J_5	0.0090	0.0089	0.0181	0.5852
J_6	0.0189	0.0187	0.0310	0.9615
J_7	0.1268	0.1279	0.1471	0.4538

Table 2. Performance indices of the random unevenness disturbance case.

In the second scenario a bump on the road is simulated as seen in Figure 8. In this case, the VSC controllers have a similar performance and it happened in the previous scenario. The performance indices of Table 3 confirm this fact. In comparison, the σ_3 controller seems to perform slightly better, specially at reusing the peak response of the suspicion and tyre deflections as can be seen in Figure 10 and 11 where a comparison between then σ_3 and backstepping controllers is illustrated. These results are in the line than those of the first scenario. It is worth noting the fact that the VSC controllers perform better with less control effort.

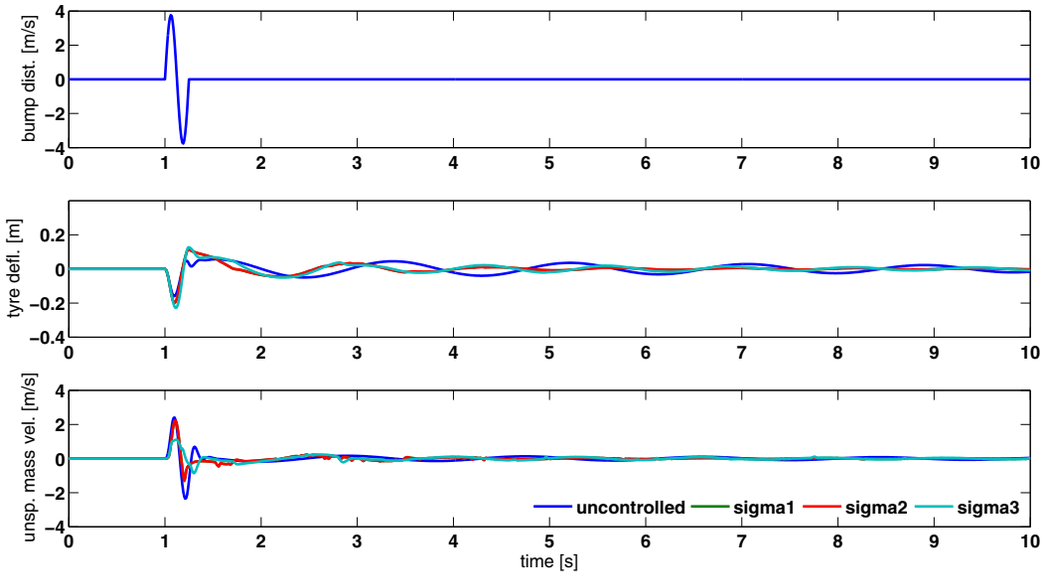

Figure 8. Bump on the road disturbance and tyre subsystem response.

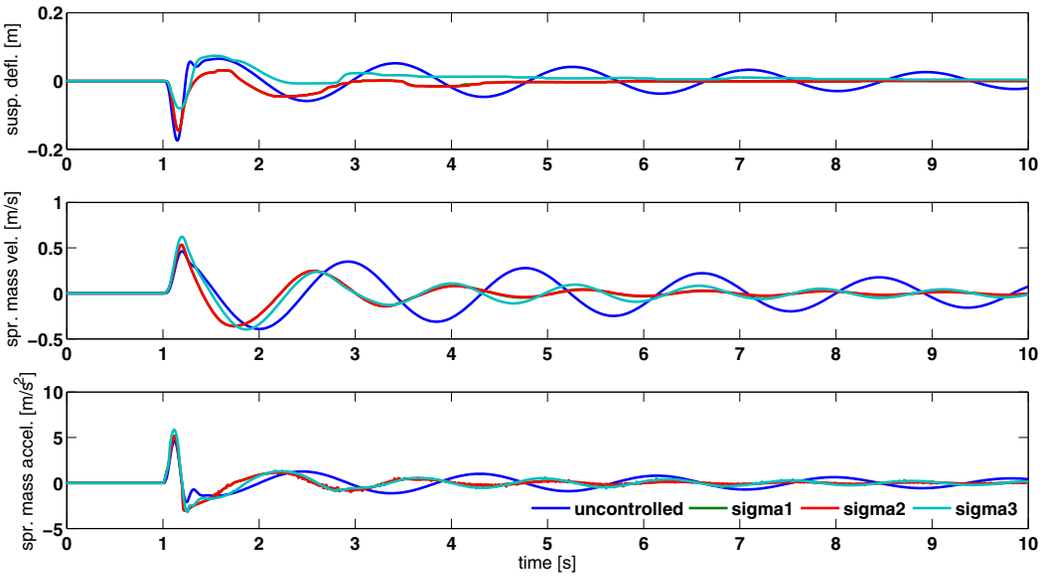

Figure 9. Bump on the road disturbance and tyre subsystem response.

Index	σ_1	σ_2	σ_3	Backstepping
J_1	0.8317	0.8325	0.4584	0.4271
J_2	1.1507	1.1505	1.3430	1.3892
J_3	1.1157	1.2623	1.2623	1.3007
J_4	0.1605	0.1625	0.2241	0.0703
J_5	0.1827	0.1797	0.2681	0.4702
J_6	0.4168	0.4113	0.5884	1.0308
J_7	0.3613	0.3614	0.4100	0.4431

Table 3. Performance indices of the road bump disturbance case.

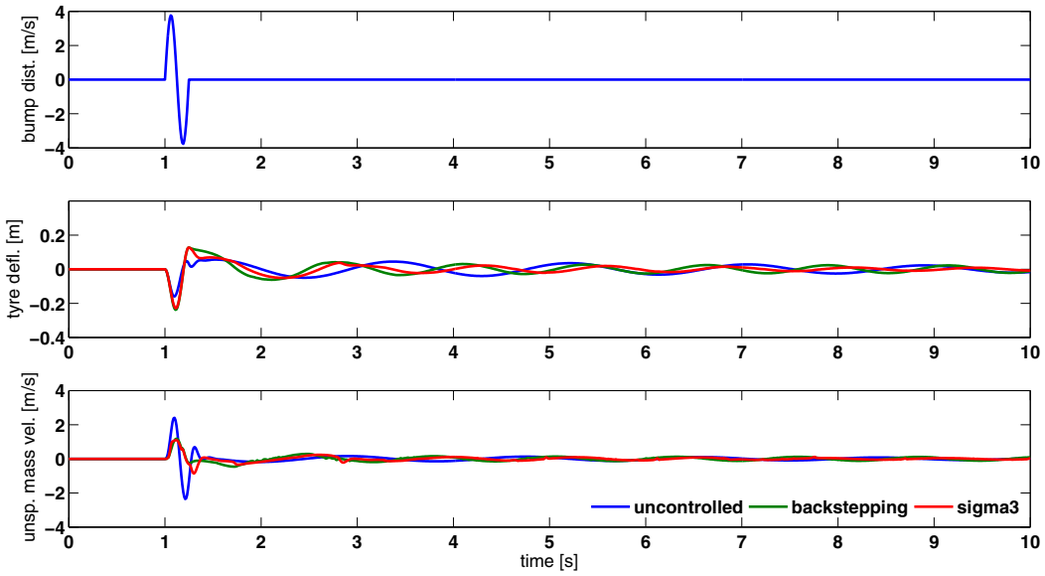

Figure 10. Bump on the road disturbance and tyre subsystem response.

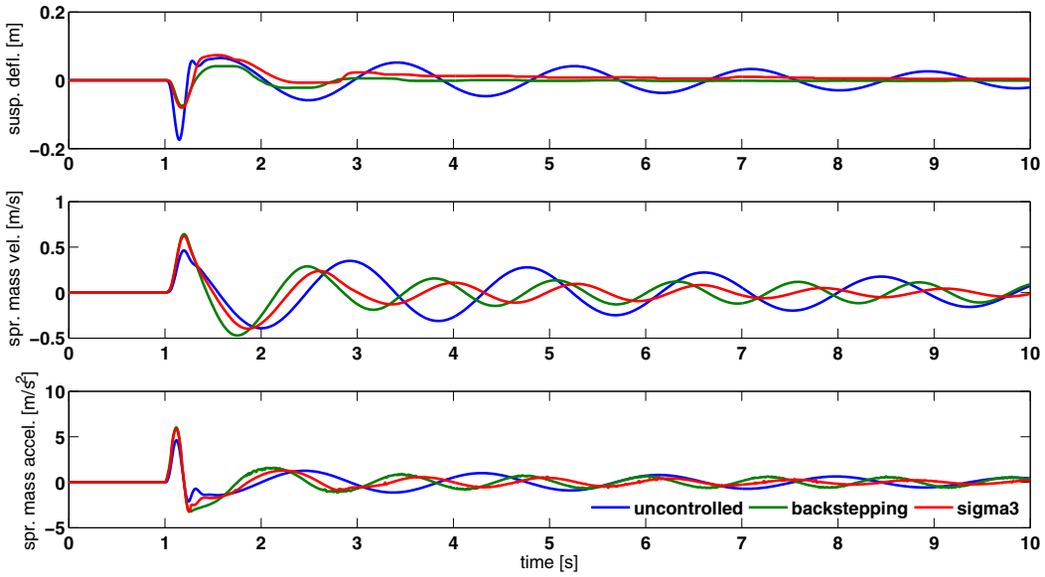

Figure 11. Bump on the road disturbance and car subsystem response.

6. Conclusions

In this chapter we presented the problem of the vibration control in vehicles. One model-based and three variable structure controllers were analyzed and compared in order to study their performance during typical road disturbances. The performance of the controller were also analyzed for the particular situation in which the suspension system is made up of a magnetorheological damper, which is well-known to be a nonlinear device. All of the controllers performed satisfactorily at regulating the suspension deflection while keeping the acceleration, velocity and displacement variables within acceptable limits. One important result obtained in this work was that despite the simplicity of these controllers, they performed significantly better than the model-based controller. It is to be noted that further studies -theoretical and experimental- should be performed in order to get a better insight of the performance of such controllers and the possibilities of being used in real systems.

Acknowledgements

M. Zapateiro has been supported by the 'Juan de la Cierva' fellowship from the Government of Spain. This study has also been partially supported by Secretaría de Estado de Investigación, Desarrollo e Innovación (formerly, Ministry of Science and Innovation) through DPI2011-27567-C02-02, DPI2011-28033-C03-01 and DPI 2011-27567-C02-01.

Author details

Mauricio Zapateiro and Francesc Pozo
Department of Applied Mathematics III, Universitat Politècnica de Catalunya, Barcelona, Spain

Ningsu Luo
Institute of Informatics and Applications, University of Girona, Girona, Spain

7. References

[1] A.M. Amani, A.K. Sedigh, M.J. Yazdampanah. A QFT approach to robust control of automobiles active suspension, *2004 5th Asian Control Conference*, Melbourne, Australia, 2004.

[2] A. Bahar, F. Pozo, L. Acho, J. Rodellar, A. Barbat. Hierarchical semi-active control of base-isolated structures using a new inverse model of magnetorheological dampers, *Computers and Structures*, Vol. 88, pp. 483-496, 2010.

[3] O. Barambones and P. Alkorta, A robust vector control for induction motor drives with an adaptive sliding-mode control law, *Journal of The Franklin Institute*, vol. 348, no. 2, pp. 300–314, 2011.

[4] M. Braci, S. Diop. On numerical differentiation algorithms for nonlinear estimation, *Proc. of the 42nd IEEE Conference on Decision and Control*, Hawaii, USA, 2003.

[5] J. Carrion, B.F. Spencer, Jr. Model-based strategies for real-time hybrid testing, *Technical Report, University of Illinois at Urbana-Champaign*, Available at: http://hdl.handle.net/2142/3629, 2007.

[6] C.Y. Chen, M.H.M. Chen, C.H. Lee. Backstepping controller design for a manipulator with compliance, *ICIC Express Letters*, vol. 4, no. 5(A), pp. 1723-1728, 2010.
[7] S.-L. Chen, C.-C. Weng. Robust control of a voltage-controlled three-pole active magnetic bearing system, *IEEE/ASME Transactions on Mechatronics*, Vol. 15, no. 3, pp. 381-388, 2010.
[8] H. Du, K.Y. Sze, J. Lam. Semi-active H_∞ control of vehicle suspension with magneto-rheological dampers, *Journal of Sound and Vibration*, vol. 283, pp. 981-996.
[9] S.J. Dyke, B.F. Spencer, M.K. Sain, J.D. Carlson. Modeling and control of magnetorheological dampers for seismic response reduction, *Smart Materials and Structures*, vol. 5, no. 5, pp. 565–575, 1996.
[10] W. Gao and J.C. Hung. Variable structure control of nonlinear systems: a new approach, *IEEE Transactions on Industrial Electronics*, vol. 40, no. 1, pp. 45–55, 1993.
[11] H. Gao, W. Sun, P. Shi. Robust sampled-data H_∞ control for vehicle active suspension systems, *IEEE Transactions on Control Systems Technology*, vol. 18, no. 1, pp. 238–245, 2010.
[12] V.Y. Glizer, V. Turetsky, L. Fridman, and J. Shinar. History-dependent modified sliding mode interception strategies with maximal capture zone, *Journal of The Franklin Institute*, vol. 349, no. 2, pp. 638–657, 2012.
[13] N. Karlsson, A. Teel, D. Hrovat. A backstepping approach to control of active suspensions, *Proceedings of the 40th IEEE Conference on Decision and Control*, Orlando, Florida, USA, 2001.
[14] M. Krstic, I. Kanellakopoulos, O. Kokotovic. *Nonlinear and Adaptive Control Design*, John Wiley and Sons, Inc., 1995.
[15] C. Liu, S, Tong, Y. Li, Adaptive fuzzy backstepping output feedback control for nonlinear systems with unknown sign of high-frequency gain, *ICIC Express Letters*, Vol. 4,no. 5(A), pp. 1698-1694, 2010.
[16] T.T. Nguyen, T.H. Bui, T.P. Tran, S.B. Kim. A hybrid control of active suspension system using H_∞ and nonlinear adaptive controls, *IEEE International Symposium on Industrial Electronics*, Pusan, Korea, 2001.
[17] M.C. Pai. Design of adaptive sliding mode controller for robust tracking and model following, *Journal of The Franklin Institute*, vol. 347, no. 10, pp. 1837–1849, 2010.
[18] M.M. Rashid, N. A. Rahim, M.A. Hussain, M.A. Rahman. Analysis and Experimental Study of Magnetorheological-Based Damper for Semiactive Suspension System Using Fuzzy Hybrids, *IEEE Transactions on Industry Applications*, vol. 47, no. 2, pp. 1051–1059, 2011.
[19] B.F. Spencer, Jr., S.J. Dyke, M. Sain, J.D. Carlson, Phenomenological model of a magnetorheological damper, *ASCE Journal of Engineering Mechanics*, Vol. 123, pp. 230-238, 1997.
[20] T.T Soong and B.F. Spencer Jr. Supplemental energy dissipation: state-of-the-art and state-of-the-practice, *Engineering Structures*, vol. 24, no. 3, pp. 243–259, 2002.
[21] W. Sun, H. Gao, O. Kaynak. Finite Frequency H_∞ Control for Vehicle Active Suspension Systems, *IEEE Transactions on Control Systems Technology*, vol. 19, no. 2, pp. 416–422, 2011.
[22] S. Tong, Y. Li, T. Wang. Adaptive fuzzy backstepping fault-tolerant control for uncertain nonlinear systems based on dynamic surface, *International Journal of Innovative Computing, Information and Control*, Vol. 5, no. 10(A), pp. 3249-3261, 2009.

[23] E.R. Wang, X.Q. Ma, S. Rakheja, C.Y. Su. Semi-active control of vehicle vibration with MR-dampers, *Proc. of the 42nd IEEE Conference on Decision and Control*, Maui, Hawaii USA, 2003.

[24] T. Wang, S. Tong, Y. Li. Robust adaptive fuzzy control for nonlinear system with dynamic uncertainties based on backstepping, *International Journal of Innovative Computing, Information and Control*, Vol. 5, no. 9, pp. 2675-2688, 2009.

[25] G.Z. Yao, F.F: Yap, G. Chen, W.H. Li, S.H. Yeo. MR damper and its application for semi-active control of vehicle suspension system, *Mechatronics*, vol. 12(7), pp. 963-973.

[26] M. Zapateiro, N. Luo, H.R. Karimi, J. Vehí. Vibration control of a class of semiactive suspension system using neural network and backstepping techniques, *Mechanical Systems and Signal Processing*, Vol. 23, 1946-1953, 2009.

[27] M. Zapateiro, H.R. Karimi, N. Luo, B.F. Spencer, Jr. Real-time hybrid testing of semiactive control strategies for vibration reduction in a structure with MR damper, *Structural Control and Health Monitoring*, Vol. 17(4), pp.427-451, 2010.

[28] M. Zapateiro, F. Pozo, H.R. Karimi, N. Luo, Semiactive control methodologies for suspension control with magnetorheological dampers, *IEEE/ASME Transactions on Mechatronics*, vol. 17(2), pp. 370-380, 2012.

[29] Z. Zexu, W. Weidong, L. Litao, H. Xiangyu, C. Hutao, L. Shuang, and C. Pingyuan. Robust sliding mode guidance and control for soft landing on small bodies, *Journal of The Franklin Institute*, vol. 349, no. 2, pp. 493–509, 2012.